Fatigue of clamped connections with application to a stem-handlebar assembly for off-road bicycles

S. P. McKENNA, M. R. HILL and M. L. HULL
Department of Mechanical and Aeronautical Engineering, University of California, One Shields Avenue, Davis, CA 95616, USA

Received in final form 17 June 2002

ABSTRACT The objectives of this study were: (i) to determine the stresses as a result of assembly and the stress concentration of a clamped connection, (ii) to demonstrate the importance of the effects of assembly in fatigue life predictions and (iii) to verify the accuracy of fatigue life predictions by measuring fatigue life experimentally. A stem-handlebar assembly used in off-road bicycles was chosen for the study because it is a critical assembly for which structural reliability must be insured to prevent serious injury. Assembly stresses in the handlebar exceeded 200 MPa and stress concentration because of the attached stem increased the applied stress by 40%. A stress-life prediction indicated that assembly effects would reduce predicted fatigue life of the handlebar by a factor of approximately 20. The measured fatigue lifetime of the handlebar was longer than that predicted by using the stress-life approach, but was much shorter than that predicted when assembly effects were ignored. Therefore, assembly effects have a significant effect on fatigue life predictions and should be included in lifetime assessments for clamped mechanical assemblies.

Keywords bicycle; clamped assembly; fatigue; handlebar; stress concentration; assembly stress.

NOMENCLATURE

X = coordinate direction ahead of the bicycle, parallel to ground
Z = coordinate direction normal to X, upward from ground
θ_b = angle in the X–Z coordinate system, measured from X
α = angle of loading, with same sense as θ_b
R = load ratio, stress ratio
ε_L, ε_T = strains along (L) and perpendicular to (T) the handlebar axis
σ_L, σ_T = normal stress components along (L) and perpendicular to (T) the handlebar axis
E, ν = Young's modulus and Poisson's ratio
σ_N = normalized bending stress
W = weight applied near the end of the handlebar
L = distance from applied load (moment arm)
r_o = outer radius of the handlebar
I = moment of inertia of the handlebar cross section
B_X, B_Z = normalized bending stress as a result of a force along the X or Z direction
F_X, F_Z = force applied in the X or Z direction
σ_{app} = stress as a result of applied load
B_α = normalized bending stress as a result of a force applied at angle α
$\sigma_{m,ass}$ = effective assembly stress
σ_{Tot} = total stress; sum of applied stress and effective assembly stress
σ_{max} = maximum total stress
σ_{eq} = equivalent stress in fatigue
N_f = cycles to failure

Correspondence: Prof. Michael R. Hill, Department of Mechanical and Aeronautical Engineering, University of California, One Shields Avenue, Davis, CA 95616, USA. E-mail: mrhill@ucdavis.edu

INTRODUCTION

One common type of mechanical connection used in order to assemble structural components is a clamped connection, which can affect the fatigue performance of the assembled structural components. Examples of clamped connections include the joining of a hub to a shaft by using a set screw, the attachment of a hub to a shaft by using a clamp, the securing of piping by using a yoke and the attachment of a bicycle handlebar to its stem via a pinch clamp (Fig. 1). In all the clamped connections shown in Fig. 1, the tightening of the securing fastener(s) produces assembly stress in the assembled structural components. Further, because these connections are also a point of support and/or a change in cross-section, stress concentration will also occur. These two effects of clamped assembly affect both the mean and amplitude values of cyclic stress and hence will influence fatigue performance of the assembled structural components.

Though many applications demand that the clamped structural components carry significant levels of cyclic loading thus rendering the effects of assembly on fatigue performance of interest[3] there have been few previous studies on the fatigue lives of structural components in clamped assemblies. To our knowledge, only a single clamp-specific, quantitative study of the effects of assembly on fatigue performance has been reported previously.[4] This study investigated clamping a collar onto a solid cylindrical shaft and found that assembly reduced the fatigue strength of the shaft by 55% at long lifetimes. While demonstrating that assembly has a profound effect on high-cycle fatigue life of a structural component, this study did not quantify either the assembly stress per se or the stress concentration, so that no analytical prediction of the fatigue life of the assembled structural components was made. Because the analytical prediction of fatigue life would be useful in the design of structural components assembled by clamping, the general goal of the present study was to develop and verify a method for predicting high-cycle fatigue life of structural components in clamped assemblies. In order to meet this general goal, the specific objectives were as follows: (i) to quantify the effects of assembly in a fatigue-prone structural component for a particular clamped assembly, (ii) to include the assembly effects in an analytical prediction of fatigue life for that structural component and (iii) to verify the analytical fatigue life prediction with fatigue testing of that structural component.

In order to satisfy these specific objectives, a particular clamped assembly must be selected. In the off-road bicycle, clamped components play a key role in rider support and control of the bicycle. Critical clamped assemblies include the stem-handlebar, seatpost-frame and numerous similar assemblies. These clamped assemblies are critical because the structural components may experience high service loads and their failure can result in either the loss of steering and braking control or the loss of support for the rider's weight, thereby leading to serious injury. Such failures have occurred in service and have led to a number of product recalls for off-road bicycles (e.g. Refs [5, 6]). Accordingly, the handlebar in the stem-handlebar assembly was selected in order to satisfy the objectives above.

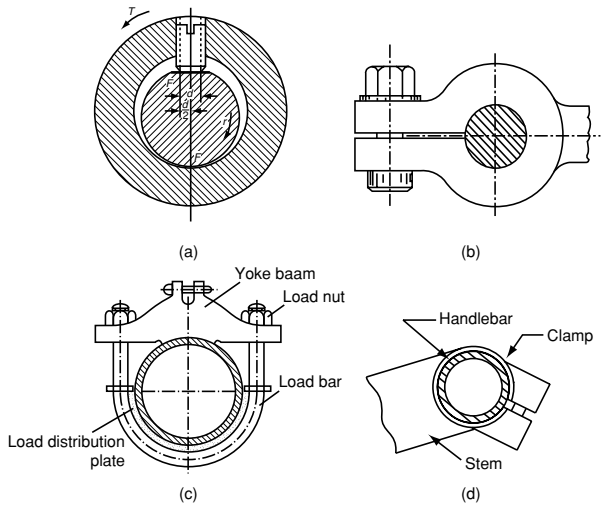

Fig. 1 Examples of mechanical assemblies: (a) hub connected to a shaft by a set screw,[1] (b) split hub,[2] (c) pipe yoke[2] and (d) bicycle stem.

METHODS

Materials

A stem and handlebar were selected from commonly available, off-road bicycle components. The stem had a one-bolt clamp (1-bolt stem), where the clamp wrapped around the handlebar and bolted together on the underside of the stem (Fig. 2a). The 1-bolt stem was made of steel and had the stem extension perpendicular to the quill. The handlebar was 580 mm long, with a cylindrical cross-section of nominal outer diameter of 25.4 mm and wall thickness of 2.2 mm. The bar had a bend of 6° (Fig. 2b) and was made of 6061-T6 aluminum (material properties given in Table 1).

Table 1 Material properties for 6061-T6 aluminum[7]

E	ν	S_y	S_u
73.1 GPa	0.345	276 MPa	310 MPa

Experiments

Assembly stress

In order to determine stress in the handlebar as a result of assembly, strain gages were mounted on the outer surface of the handlebar and measured strain change during clamping. Four, two-element, 90° strain gage rosettes were placed at 90° intervals around the circumference, so that each rosette had an element orientated in both the longitudinal and transverse – that is, circumferential – directions of the handlebar.

Assembly strain was measured at 10° increments around the stem–handlebar interface, with gage centers 1.6 mm away from the edge of the clamp. The assembly strain was measured by repeatedly tightening the stem clamp bolt with the handlebar rotated through 80°, in 10° increments, relative to the stem. In order to ensure consistency in the clamping force from tightening the stem clamp bolt, the bolt force was measured with a bolt force transducer made from a cylindrical steel sleeve instrumented with strain gages. Bolt force was measured, rather than tightening torque, because friction does not allow consistent bolt force at a given measured torque.[8] The stem clamp bolt was tightened until the bolt force transducer indicated a specific strain, corresponding to an average tightening torque of 11.4 Nm (100 in-lb).

Stress concentration

The instrumented handlebar was also used in order to quantify the stress concentration in the handlebar when loaded in bending. Because the theoretical bending stress is zero on the neutral axis, loads were applied along two orthogonal directions in order to determine the stress concentration. For each loading direction, the instrumented handlebar was rotated incrementally by 10° with respect to the stem in order to map the bending strain around the entire stem–handlebar interface. The two load directions were 287° and 197° with respect to the *x*-axis of the reference frame used in this study

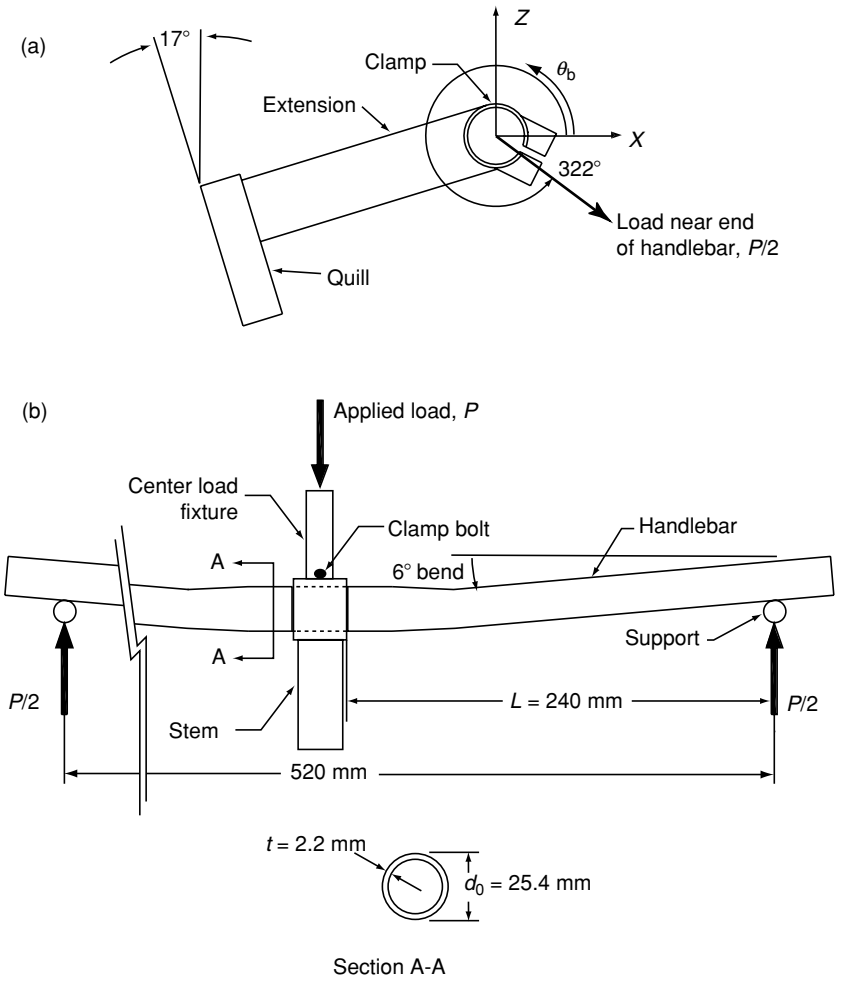

Fig. 2 Test articles and loading: (a) one-bolt stem and (b) stem-handlebar assembly with handlebar cross-section. Here, (a) also shows the *X*–*Z* coordinate frame and typical 17° head-tube angle assumed, as well as the direction of applied load used in fatigue testing (322° from the *x*-axis); (b) also shows the three-point bending used for fatigue testing, where roller supports were placed where the hands would apply loads and a centre load fixture was attached to the stem quill.

(Fig. 2a). Bending stress was produced by hanging three weights of 159, 204 and 248 N from the end of the handlebar. The bending strain data were reduced to stresses and these were compared to stresses from beam theory in order to quantify stress concentration.

Fatigue tests

Constant amplitude cyclic loads were applied by means of a servohydraulic test machine to the stem-handlebar assembly with the handlebar in 3-point bending (Fig. 2b). The middle load was applied to the stem quill and the outer loads directly to the handlebar. All testing was performed at an applied load ratio of $R = 0.1$. The span used in testing was 520 mm, so that the bar was loaded near its ends, similar to field loading.

A special test fixture was designed for the 3-point bending fatigue test. The hydraulic actuator was connected to the part of the fixture that held the stem. The handlebar rested on two rollers supported by an arm that spanned the length of the handlebar and the arm was attached to a load cell. This fixture loaded the handlebar such that the loads near the end of the handlebar were at a load angle $\alpha = 322^\circ$ relative to the x-axis (Fig. 2a). This load angle was used because a recent study of fatigue as a result of loads occurring during down-hill, off-road cycling indicated that this load angle was appropriate for a single-axis fatigue testing protocol.[9] This load direction is also similar to the loading direction used in another recent study[10] to rank stems for fatigue performance.

In order to map the load-life curve for the handlebar, five load ranges (maximum load = 1.2, 1.4, 1.7, 1.89 and 2.1 kN) were used in order to obtain lifetimes between 10^4 and 10^6 cycles. Five replicate samples were tested at each load range.

In order to ensure that most of the test cycles were required to initiate, rather than propagate, a fatigue crack, a compliance-based failure criterion was implemented. Fatigue tests were terminated when the load-line compliance (as indicated by the displacement of the hydraulic actuator) increased 10% compared to the compliance at the beginning of the test.

Data analysis

Assembly stresses

Longitudinal (σ_L) and transverse (σ_T) stresses were computed from the strains measured at various points around the circumference of the handlebar. The material response was assumed to be elastic and in plane stress, so that stresses were computed from:

$$\sigma_L = \frac{E(\varepsilon_L + v\varepsilon_T)}{1 - v^2} \quad (1)$$

$$\sigma_T = \frac{E(\varepsilon_T + v\varepsilon_L)}{1 - v^2} \quad (2)$$

where E is the modulus of elasticity, v is Poisson's ratio, ε_T is the measured transverse strain and ε_L is the measured longitudinal strain.

Stress concentration

Stress concentration was quantified by using normalized bending stress. Because the stress concentration factor is undefined on the neutral axis, it was not a useful quantity in the present study. The normalized bending stress σ_N was computed as the ratio of the longitudinal stress to the maximum bending stress determined from beam theory in the absence of assembly effects:

$$\sigma_N(\alpha, \theta_b) = \left(\frac{I}{WLr_o}\right) \sigma_L(\alpha, \theta_b) \quad (3)$$

where W is the weight applied to the end of the bar for a given value of σ_L, L is the distance from the point of load application to the edge of the stem, I is the moment of inertia of the handlebar cross-section, and r_o is the outer radius of the handlebar. The equation acknowledges the dependence of σ_N on the angle of loading α and on the position around the circumference of the handlebar θ_b, which arises from the geometry of the stem clamp and the distribution of the bending stress.

In order to determine the normalized bending stress within the context of the definition above, strains were measured as a result of the cantilevered loads and the corresponding longitudinal stress σ_L was calculated from Eq. (1). The normalized bending stress was determined for each of the three loads used in the experiments and these values were averaged to reduce uncertainty.

Because the normalized bending stress depended on the loading angle α, the normalized bending stress at an arbitrary angular position θ_b and arbitrary loading angle was determined from the two distributions of normalized bending stress measured in the experiments ($\alpha = 287^\circ$ and 197°). In order to aid in the comparison of the results for the 1-bolt stem with those obtained on other stems (in future work), the two normalized bending stress distributions were transformed into the reference axes (Fig. 2a). Therefore, the results for normalized bending stress are presented in terms of normalized bending stress contributions corresponding to loads applied in the X- and Z-directions. These are defined as B_X and B_Z, respectively, and were determined from the normalized stress found for the two orthogonal load axes by using a coordinate rotation:

$$B_X(\theta_b) = \sin(287^\circ)^*\sigma_N(197^\circ, \theta_b) - \sin(197)^*\sigma_N(287^\circ, \theta_b) \quad (4)$$

$$B_Z(\theta_b) = -\cos(287^\circ)^*\sigma_N(197^\circ, \theta_b) + \cos(197)^*\sigma_N(287^\circ, \theta_b) \quad (5)$$

B_X and B_Z enable the calculation of applied bending stresses around the handlebar by simply multiplying the normalized bending stress contributions by applied force components in the X- and Z-directions, the moment arm and cross-sectional properties of the handlebar:

$$\sigma_{app}(t, \theta_b) = \frac{Lr_o}{I}(B_X F_X(t) + B_Z F_Z(t)) \quad (6)$$

where $F_X(t)$ and $F_Z(t)$ are the force components applied at a distance L from the edge of the stem, as a function of time t. For the present study, which considers constant amplitude loading applied along a single direction ($\alpha = 322^\circ$), it is also illustrative to present the normalized bending stress for loading along a single direction:

$$B_\alpha(\theta_b) = B_X(\theta_b)\cos(\alpha) + B_Z(\theta_b)\sin(\alpha) \quad (7)$$

where $B_\alpha(\theta_b)$ is the normalized bending stress for the specific angle of loading α and is a function of the angular position around the handlebar θ_b.

In order to verify the superposition of the normalized bending stress contributions given in Eq. (7), the normalized bending stress also was determined experimentally with the load applied along a third angle, $\alpha = 317^\circ$ and these results were compared to the normalized stress distribution computed by using Eq. (7).

Fatigue life predictions

The assembly stress was assumed not to vary with time and was therefore treated as an effective mean stress. Because the assembly stress was biaxial, Sines's method[11] was used in order to account for the effect of assembly stress in fatigue. Sines's method relates the mean stresses in any three mutually orthogonal directions to a single, effective mean stress value:

$$\sigma_m = \sigma_{xx,m} + \sigma_{yy,m} + \sigma_{zz,m} \quad (8)$$

where σ_m is the effective mean stress and $\sigma_{xx,m}$, $\sigma_{yy,m}$, $\sigma_{zz,m}$ are the mean values of the three normal stress components during a given loading cycle. For the biaxial state on the outer surface of the stem-handlebar assembly, the effective assembly stress in fatigue, $\sigma_{m,ass}$, was determined by adding together the assembly stresses in the longitudinal and transverse directions:

$$\sigma_{m,ass}(\theta_b) = \sigma_{L,ass}(\theta_b) + \sigma_{T,ass}(\theta_b) \quad (9)$$

The total stress at each point on the handlebar was determined as the sum of the applied and effective assembly stresses:

$$\sigma_{Tot}(t, \theta_b) = \sigma_{app}(t, \theta_b) + \sigma_{m,ass}(\theta_b) \quad (10)$$

where σ_{Tot} is the total stress in the handlebar at a given time and position around the circumference. The total stress was used in subsequent fatigue life predictions in order to account for both assembly stress and applied stress as affected by stress concentration.

Failure was predicted from the cyclic stresses of Eq. (10) by using the Walker equation.[12] Fatigue lifetime was predicted at each of 360 points around the handlebar – that is, every 1° – and the shortest life was taken as the predicted lifetime for the handlebar. Linear interpolation was used in order to estimate values of the assembly stress and the normalized bending stress, which were measured every 10°. For a given level of applied loading, both the maximum stress σ_{max} and stress ratio R were determined for the point of interest by using the total stress of Eq. (10) and used in order to determine an equivalent zero-to-tension cyclic stress σ_{eq} from the Walker equation:[12]

$$\sigma_{eq}(\theta_b) = \sigma_{max}(\theta_b)(1 - R(\theta_b))^{0.63} \quad (11)$$

The equivalent stress was then used in order to estimate constant amplitude lifetime, N_f, by using:

$$N_f = \left(\frac{\sigma_{eq}(\theta_b)}{871.5\ \text{MPa}}\right)^{-9.84} \quad (12)$$

The Walker exponent (0.63) in Eq. (11) and the fatigue strength coefficient and exponent (871.5 MPa and −9.84) in Eq. (12) were previously reported[7] and were found from fatigue data for 6061-T6 over a wide range of stress ratios.

Using the above equations enabled the point of maximum damage to be predicted, accounting for the combined effects of applied external loading and assembly. The point of maximum damage for a constant amplitude cyclic load test is the location of highest equivalent stress and consequently has the shortest predicted lifetime. If assembly effects were not included, then the point of maximum damage would occur 180° from the loading direction, but assembly stress and stress concentration can alter the location of this point.

Failure analysis

For each fatigue test, the location of crack initiation was determined. The location of crack initiation was important because it showed the location of the maximum localized stress as influenced by various factors such as specimen variations, fretting and proximity to grooves in the handlebar. The location of crack initiation was determined by observing the fracture surface under magnification and noting where the crack initiated. Using

intervals of 5°, a histogram of the locations of crack initiation was used in order to experimentally determine the location of highest stress, which was compared to the location of maximum damage predicted by using the Walker equation.

RESULTS

Assembly stress

The magnitudes of the assembly stresses in the longitudinal and transverse directions varied depending on the location around the handlebar (Fig. 3). The longitudinal assembly stress was generally positive with local peaks of 92.5 and 104.3 MPa occurring at $\theta_b = 147°$ and 327°, respectively (Fig. 3). The minimum longitudinal stresses of −2.8 and −15.3 MPa occurred at 47° and 207°. Transverse stresses resulted from the effects of secondary bending caused by clamping which distorted the cross-sectional shape from circular (e.g. oval). As a result, the transverse stress was either positive or negative depending on the angular position. The maximum transverse stress of 116.7 MPa occurred at 287° and the minimum of −197.1 MPa occurred at 197° relative to the *x*-axis.

Stress concentration

In order to appreciate the stress concentration induced by the stem-handlebar assembly, the normalized bending stress contributions at each point around the handlebar circumference were computed and were compared to the stress contributions at each point as a result of beam theory – that is, no stress concentration. If no stress concentration were present, then B_X would be equal to negative cosine and B_Z would be equal to negative sine (Fig. 4). The discrepancies between the actual normalized stresses and their corresponding theoretical trigonometric functions are an effect of the stem-handlebar assembly. The largest value for B_X was 1.41 at 187°; the largest value of B_Z, was 1.32 at 247°.

The measured normalized bending stress for a load along $\alpha = 317°$ agreed closely with the results of Eq. (7) (Fig. 5). This confirmed that the normalized bending stresses determined with loads along two orthogonal axes provided adequate information in order to estimate stresses in the handlebar with the load applied along an arbitrary load angle. Therefore, B_X and B_Z were sufficient to map out the bending stress under loading along an arbitrary direction.

Comparison of the normalized bending stress for the direction of loading used in fatigue testing ($\alpha = 322°$) demonstrated the stress concentration unique to the stem-handlebar assembly (Fig. 6). With no assembly effects, the stress would be equal to 1.0 at $\theta_b = 142°$. Owing to assembly, however, the maximum normalized bending stress was 1.39 at $\theta_b = 177°$. Effects from assembly shifted the location of the maximum bending stress by 35°. The maximum normalized bending stress occurred in the region of the stem reinforced by the stem extension (Fig. 6).

Fatigue life predictions

Assembly effects significantly influenced the fatigue life prediction of the handlebar. The predicted point of

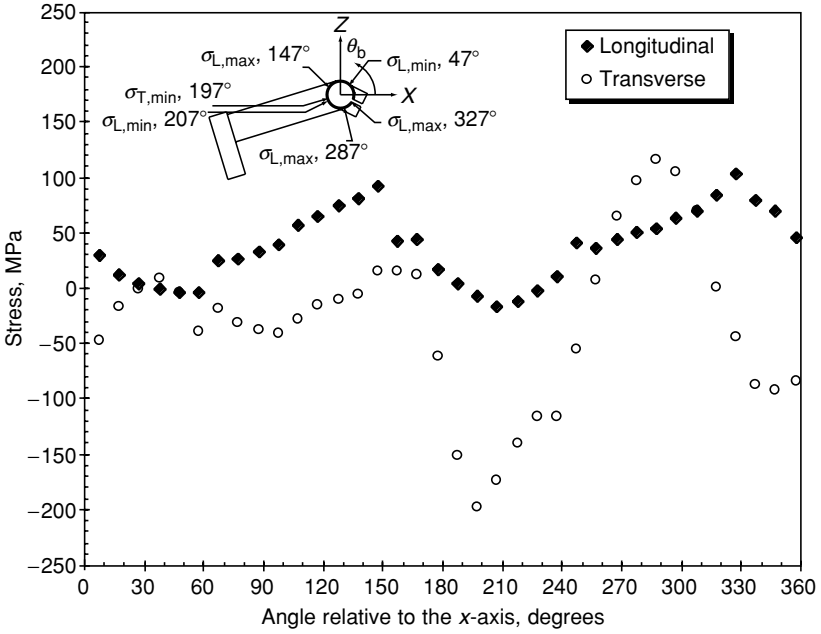

Fig. 3 Longitudinal and transverse assembly stress in the handlebar as a function of the angle relative to the *x*-axis. Inset shows the location of assembly stress extrema. Results are for a bolt force equivalent to a clamping torque of 11.4 Nm.

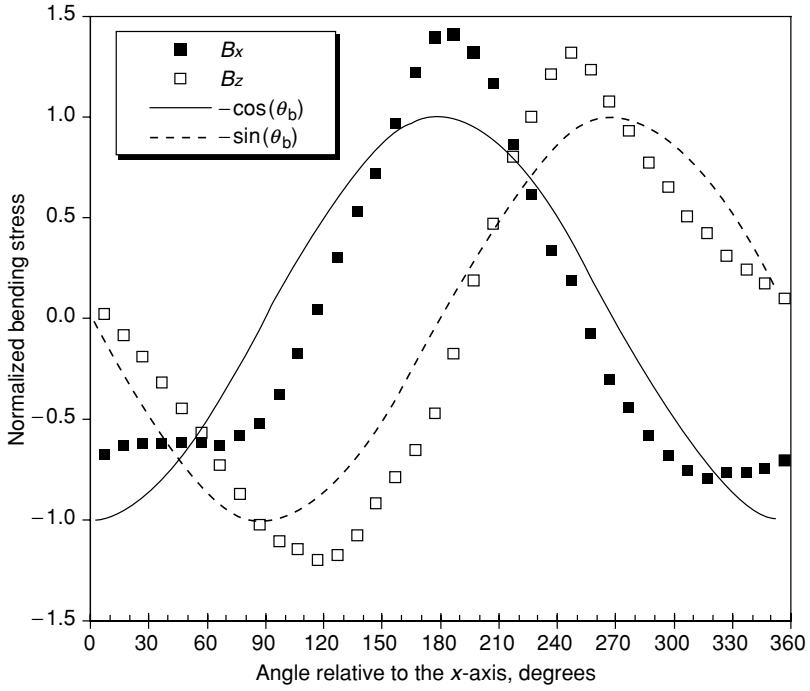

Fig. 4 Normalized bending stress in the handlebar for loads along the X and Z directions and normalized bending stress from beam theory in the absence of stress concentration.

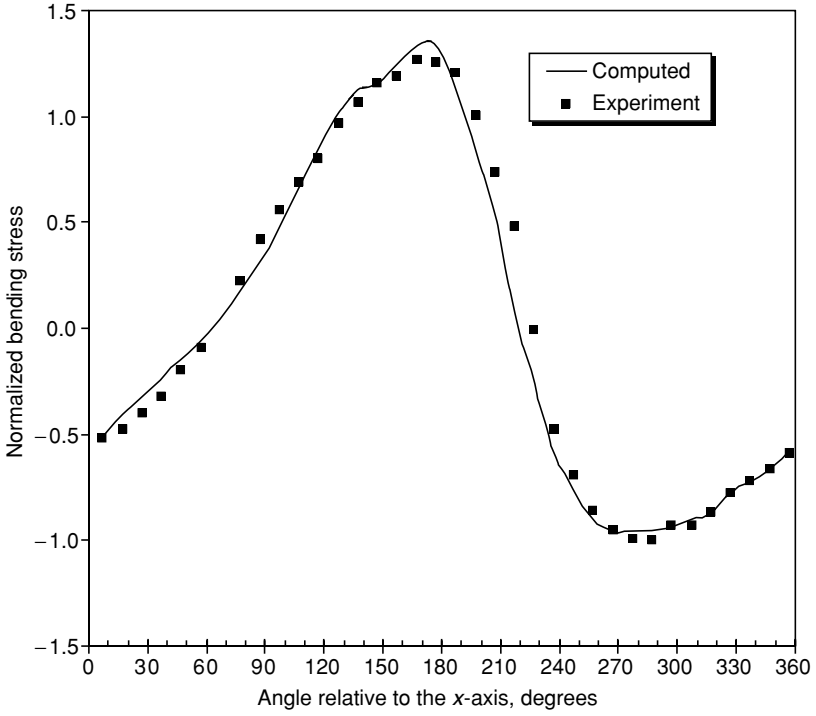

Fig. 5 Normalized bending stress in the handlebar measured for $\alpha = 317^\circ$ and computed from Eq. (7).

maximum damage for the constant amplitude cyclic loading occurred at the point of highest equivalent stress (and consequently the point of shortest lifetime). When stem effects were included in the calculation, the point of maximum damage was 167° (Fig. 7). At the point of maximum damage, the assembly effects created an elevated stress state that resulted in a shorter predicted fatigue life than the lifetime predicted without assembly effects. For an applied maximum load of 1700 N, assembly effects reduced lifetime by a factor of 18 (Fig. 8) and shifted the point of maximum damage by 25° (Fig. 7), compared to when the assembly effects were ignored.

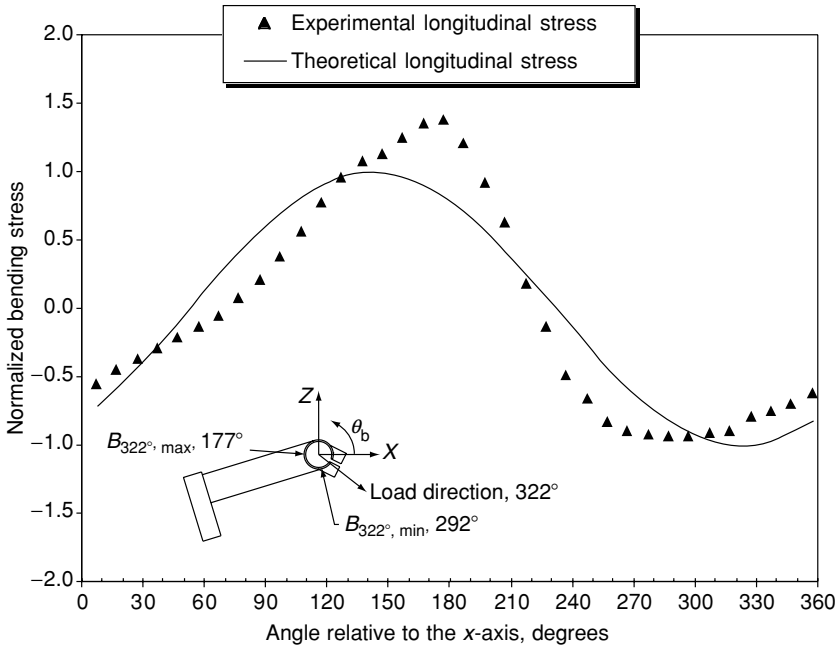

Fig. 6 Normalized bending stress in the handlebar for $\alpha = 322^\circ$ and normalized bending stress from beam theory. Inset shows the location of normalized bending stress extrema.

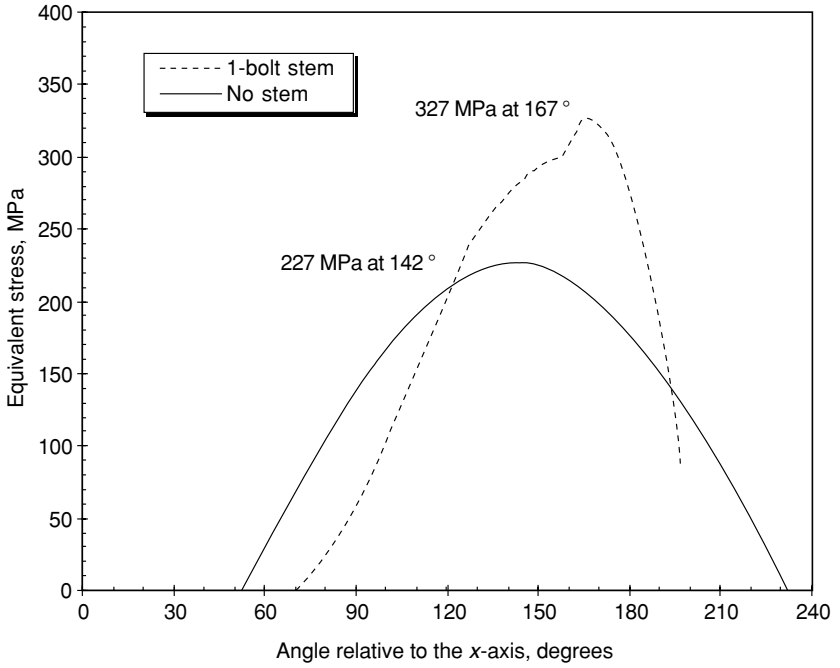

Fig. 7 Equivalent stress in the handlebar as a function of θ_b for the stem-handlebar assembly compared to beam theory. Calculated for $P_{max} = 1.7$ kN, $P_{min} = 0.17$ kN, $\alpha = 322^\circ$ and $L = 240$ mm.

Fatigue tests

Fatigue test data showed that the handlebar had a longer life than that predicted for nearly all levels of loading, but had a shorter life than that predicted without including the assembly effects (Fig. 8). The assembly effects significantly reduced the fatigue lifetimes at the point of maximum damage for all levels of stress. Deviations from the life predicted with assembly effects increased as the maximum stress (force) increased, with the prediction having an increasingly shorter life – that is, conservative. Examination of fracture surfaces suggested that most cracks nucleated at 170° (Fig. 9), which was only 3° different from (or 0.7 mm away from) the predicted point of maximum damage of 167°.

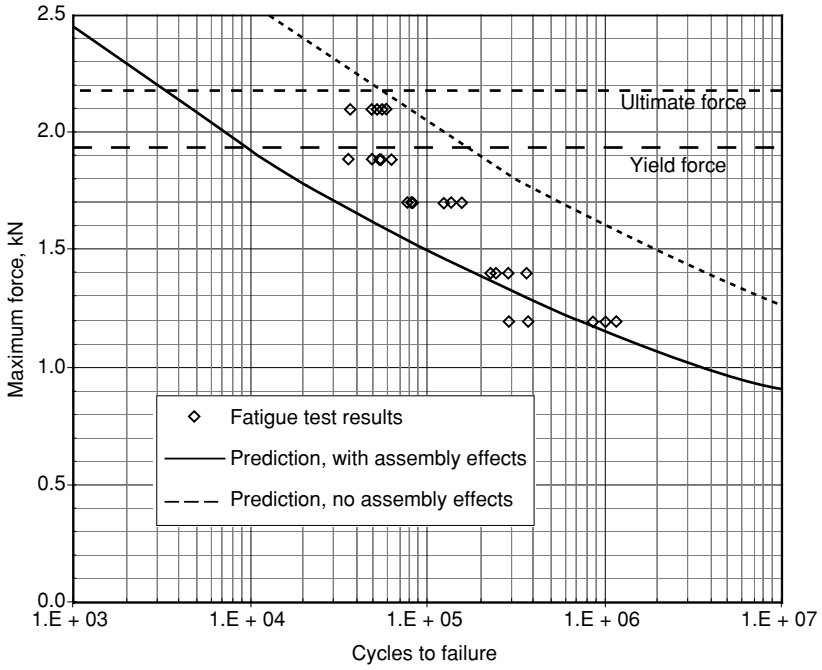

Fig. 8 Experimental and predicted fatigue life of the handlebar assembled with the stem. Tests were conducted for $\alpha = 322°$, $L = 240\,\text{mm}$ and $R = 0.1$.

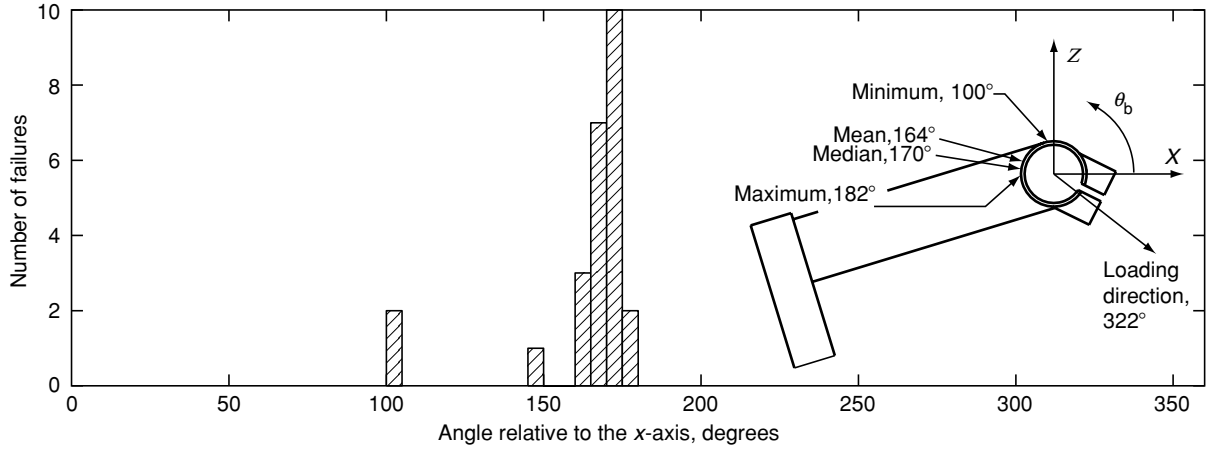

Fig. 9 Histogram of the locations of failure initiation in the handlebar. The median angle for failure initiation was 170°. Inset shows locations of statistics on the stem.

DISCUSSION

In order to prevent structural failure of the handlebar in the off-road environment, which could lead to serious injury, this study was intended to assist in the design and qualification of the stem-handlebar assembly. In order to provide this assistance, this study had three objectives. The first objective was to determine the assembly stress and normalized bending stress in the handlebar from assembly; the second objective was to analytically predict the constant amplitude load fatigue life of the handlebar both with and without assembly effects; and the third objective was to experimentally determine the high-cycle constant amplitude load fatigue life of the handlebar with the stem clamped. The key findings were:

1 The assembly introduced effects in the form of mean stresses and stress concentration that were large enough to substantially affect the predicted fatigue life of the handlebar.
2 The experimental results from the constant amplitude load fatigue tests were bracketed by predictions ignoring and including the assembly effects, with the prediction including the assembly effects being conservative.

Before discussing the importance of these results, several issues associated with the methodologies used in order to obtain these results merit critical examination.

Methodological issues

In order to quantify assembly effects, the stem bolt was tightened consistently. Manufacturers recommend a tightening torque of 9.0–11.4 Nm (80–100 in-lb). In order to generate the maximum assembly stress and hence the most conservative fatigue life prediction, we used 11.4 Nm for all experimental procedures. In order to ensure consistent clamping, a bolt force transducer was employed instead of relying on measured tightening torque.

Presumably, the effect of stress concentration would be greatest at the edge of the interface between the stem clamp and handlebar, and the concentrated stress would vary around the handlebar. In order to determine the concentrated stresses at a point on the outer surface of the handlebar close to the stem in two directions, small strain gage rosettes were mounted onto a handlebar. Physical limitations kept the midpoint of the strain gages 1.6 mm away from the edge of the stem. Therefore, the maximum magnitude of the concentrated stresses, as quantified by the normalized bending stress, may have been underestimated.

In order to account for the assembly stress effect in fatigue life predictions, several assumptions were made. First, the stress-life approach was adopted and this assumed elastic material behaviour. This method was selected because it was simple to implement, because it is widely employed in the bicycle industry and because it was capable of predicting the effects of assembly at the long lifetimes exhibited in bicycle components. Second, the assembly stress was considered to be a stress that remained constant while the applied loading fluctuated. Third, Sines's method was used in order to account for the measured biaxial assembly stress.[11] This method was chosen over a mean von Mises stress because it often provides a better match to experimental fatigue data when the mean stress components are of opposite sign[13] as in the present case (Fig. 3).

Because the assembly stress alters the mean stress differently at various positions around the handlebar, a method had to be selected for predicting the fatigue life that considered the effects of the mean stress on the life prediction. The Walker equation was selected because it gave a better fit to the reference fatigue data[7] than did other mean-correction equations (e.g. Goodman[14] and SWT[15]). In principle, other mean-corrections could be applied and should lead to similar results.

Three-point loading was used in order to apply bending loads to the handlebar, which mimics field loading in off-road cycling. A bicycle rider loads the handlebar with his/her hands toward the end of the handlebars, suggesting the wide span of the loading used (Fig. 2b).

In order to simplify the design of the test fixture, it was loaded only in compression. In order to maintain a compressive load during constant amplitude load testing, a stress ratio $R > 0$ was selected for testing. However, typical off-road bicycle loading exhibits both compressive and tensile loads. Results at other stress ratios may show either smaller or larger effects of assembly than those found at $R = 0.1$.

In order to terminate each fatigue test, a criterion based on the compliance change of the specimen was used. The initial compliance was calculated at the start of each experiment and the experiment was terminated when the initial compliance increased 10%. It was found that the test specimens spent at least 97% of their fatigue life before a visible crack was present. This implies that at most 3% of the reported fatigue life was spent in crack growth.

Importance and interpretation of results

Assembly stresses and stress concentration because of stem clamping must be considered when calculating the stresses in the handlebar. Assembly stresses depend on the position around the handlebar and the bolt tightening force. The stress concentration, quantified by using normalized bending stress, depends on the position around handlebar and the angle of loading applied. The assembly effects shifted the predicted point of maximum damage (and maximum equivalent stress) by 25° for the loading direction used in this study ($\alpha = 322°$) from $\theta_b = 142°$ to $\theta_b = 167°$. At 167°, assembly effects increased the nominal applied stress by 36% ($B_{322°} = 1.36$) and increased the mean stress by 57.7 MPa. Quantification of the two assembly effects enabled more accurate modelling of the stress state produced in the handlebar.

Both the assembly stress and normalized bending stress were elevated in the vicinity of $\theta_b = 167°$ because the stem clamp was reinforced by the stem extension in this vicinity. Here, the handlebar deformation is more restrained than in other areas. The material in this vicinity therefore resisted bending deformation and experienced an elevated stress state (stress concentration).

The maximum normalized bending stress of 1.41 determined in this study was lower than what might be expected by assuming a single part of similar geometry. Handbook stress concentration factors rely on dimensionless ratios, and for the present stem and handlebar the closest geometries were those of a solid stepped shaft in bending or a hollow stepped shaft in tension.[16] The ratio of the outer diameter of the stem to that of the handlebar was approximately 1.2. The stem did not

contain a radius per se, but the edge was rounded such that a reasonable approximation for the fillet radius to handlebar outer diameter ratio was 0.05. With these ratios, handbook[16] stress concentration factors range from 1.6 to 1.8, which is significantly larger than was found experimentally (1.41). The difference may be attributed to many factors such as differences in fillet geometry or differences in the number of parts (because the stem-handlebar assembly was two parts, it was possible for the stem clamp to deform independently of the handlebar, thereby altering stress concentration). The difference may also be a result of the small distance between the edge of the stem clamp and the strain gages used for estimating the stresses near the edge of the stem.

Experimental fatigue results for constant amplitude loading were bounded by fatigue life predictions, which included and ignored the assembly effects (Fig. 8). The effects of assembly acted to increase the equivalent stress and decrease predicted life. The fatigue life predicted with the stem effects was shorter than the experimental life and the prediction converged with the data at lower levels of loading (Fig. 8). This may be attributed to localized plasticity occurring at higher loads, with the deformation being elastic at lower loads. Because the fatigue prediction was based on elastic behaviour – that is, superposition of applied and assembly stresses and the use of static loads for stress concentration determination – the lack of agreement at higher loads is not surprising.

The median location of crack initiation in the constant amplitude load tests was close to the predicted point of maximum damage. The assembly effects were predicted to shift the location of crack initiation by 25°, relative to what would be expected from beam theory, from 142° to 167°. The fracture surfaces exhibited a median failure location of 170° (Fig. 9). Several factors were not accounted for in the fatigue prediction, but were present in the fatigue tests, including fretting, material inhomogeneity and proximity to grooves (Fig. 10a). Despite these effects, the difference between the predicted and experimental failure locations was small. In fact, the spacing between the grooves was 7° (Fig. 10a), or about twice the difference between the predicted and experimental failure locations. The large difference between the actual failure location and the location predicted by beam theory (142°) underlines the importance of assembly effects in influencing the fatigue performance of the handlebar.

Fatigue cracks in the experimental fatigue test initiated near the edge of knurling grooves, often near a region of fretting. All specimens had some signs of fretting as a result of relative motion between the stem clamp and the handlebar (Fig. 10a). A photograph taken normal to a typical fracture surface indicates that fatigue failure initiated at the outside surface because the markings in this picture point back to the location of fatigue crack initiation (Fig. 10b). The most common location for failure initiation was near the end of the grooves in the handlebar (Fig. 10). These grooves, included in the design in order to reduce slip between the handlebar and stem, induced a stress concentration at their end, which further elevated the applied stress and made the end of the groove especially prone to failure. Because the stem clamp bolt is typically tightened to 11.4 Nm, the

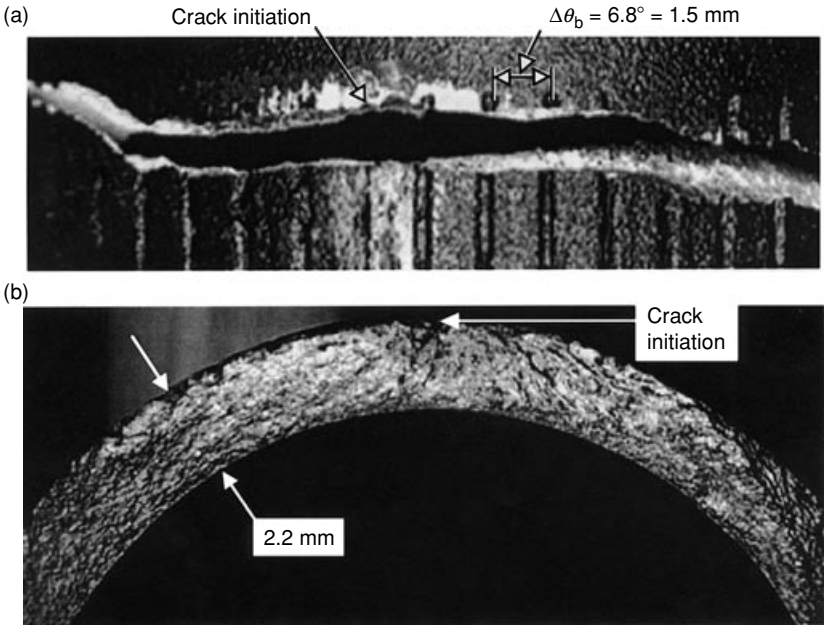

Fig. 10 Here (a) outer surface of a failed handlebar and (b) fracture surface of the handlebar shown in (a).

corresponding clamping force is sufficient to inhibit slip of the handlebar in the stem without the grooves. It may therefore be beneficial for the manufacturer to remove the grooves from the handlebar, which should then exhibit improved fatigue life. However, removing the grooves would increase the contact area between the stem and the handlebar and may therefore lead to an increased propensity for fretting because of reduced contact pressure. Therefore, the effect of removing the grooves would need to be verified by fatigue testing.

The stem clamp assembly effects significantly reduced the constant amplitude load fatigue performance of the handlebar. The predictions indicate that stem clamping reduced the fatigue strength of the handlebar by 28% at a life of 10^7 cycles (Fig. 8). In terms of fatigue lifetime, the predictions suggest that clamping reduced life by a factor of approximately 20 (Fig. 8). A previous experimental study by Lea[4] also found significant effects as a result of clamping. That study employed 6.4 mm diameter shafts loaded in rotating bending where heavy cylindrical split collars (3.8 mm wide and 28.6 mm outer diameter) were clamped at the shaft mid-span. Tests both with and without the clamped collars showed that clamping reduced the rotating bending fatigue strength 55% at a life of 10^7 cycles. The smaller effect of assembly on fatigue performance found in the present study is likely because of greater compliance of both the hollow handlebar and the stem clamp, compared to the solid shaft and heavy collar used by Lea.

The above results suggest that handlebar life prediction based on simple beam theory, and ignoring the effects of assembly, would lead to nonconservative results. A simple approach to account for assembly would be to employ a fatigue strength that is 28% of the strength in plain specimens of similar material. However, the specific reduction used in design would depend on the specific handlebar, stem and tightening torque employed. Design variables such as the radius of the clamp edge, stem stiffness and the angular positions of the extension and clamp bolt would all influence the assembly effects and hence the fatigue behaviour. Therefore, in order to best account for the effects of assembly in predicting the fatigue life, the experimental approach taken here in measuring assembly and bending strains should be duplicated and then the methods presented herein should be used in order to predict the fatigue life.

CONCLUSIONS

The conclusions from this study are summarized as follows:

1 Assembly of an off-road bicycle handlebar to a stem with a pinch-clamp introduced substantial assembly stresses in both the longitudinal (104 MPa) and transverse (−197 MPa) directions. These large stresses occurred using the bolt tightening torque recommended by the manufacturer.

2 A method unique to this study was developed in order to quantify the stress concentration effect around the entire circumference of the handlebar at the stem-handlebar clamp junction and the method was validated. This method revealed that the stress concentration at the stem-handlebar clamp junction increased the applied stress by 40% and shifted the location of the maximum bending stress by 35°.

3 Assembly effects significantly influenced the fatigue life prediction of the handlebar. For an applied maximum load of 1700 N, assembly effects reduced lifetime by a factor of 18 and shifted the point of maximum damage by 25° compared to when the assembly effects were ignored. These large differences between the lifetimes and failure locations with and without assembly effects underline the importance of assembly effects in influencing the fatigue performance of the handlebar.

4 Fatigue tests of the stem-handlebar assembly revealed that the handlebar had a longer life than that predicted for nearly all levels of loading when assembly effects were considered, but had a shorter life than that predicted when assembly effects were not considered. Therefore, in order to conservatively estimate the fatigue life of a handlebar, both the assembly stresses and stress concentration must be determined and then included in fatigue life predictions.

Acknowledgements

The authors are grateful to Answer Products and in particular Scott Boyer and Rick Pedigo for the financial support of this project. We also thank Mark LaPlant of Cannondale Corporation for supplying the handlebars.

REFERENCES

1 Fuchs, H. O. and Stephens, R. I. (1980) *Metal Fatigue in Engineering*. Wiley, New York, USA.
2 Blake, A. (1985) *Design of Mechanical Joints*. Marcel Dekker, New York, USA.
3 Grover, H. J. (1966) *Fatigue of Aircraft Structures*. U.S. Government Printing Office, Washington, D.C., USA.
4 Lea, F. C. (1937) The effect of discontinuities and surface conditions on failure under repeated stress. *Engineering* **144**, 140–144.
5 US, CPSC (1995) *CPSC, Specialized Announce Bike Brake, Handlebar Recall.* Release # 95–155, U.S. Consumer Product. Safety Commission, Office of Information and Public Affairs, Washington, D.C., USA.
6 US, CPSC (2000) *CPSC, Trek Bicycle Corp. Announce Recall of Road Bikes and Handlebar Stems.* Release # 00–192, U.S. Consumer

Product. Safety Commission, Office of Information and Public Affairs, Washington, D.C., USA.
7 US, DOD (1990) *Military Handbook: Metallic Materials and Elements for Aerospace Vehicle Structures (Mil-HDBK-5f)*. U.S. Department of Defense, MIL-HDBK-5 Coordination Activity, Wright-Patterson AFB, OH, USA.
8 Almen, J. O. and Black, P. H. (1963) *Residual Stress and Fatigue in Metals*. McGraw-Hill, NY, USA.
9 McKenna, S. P., Hill, M. R. and Hull, M. L. (2002) A single loading direction for fatigue prediction and testing of off-road bicycle handlebars. *Int. J. Fatigue*. **24**, 1149–1157.
10 Tovo, R. (2001) On the fatigue reliability evaluation of structural components under service loading. *Int. J. Fatigue* **23**, 587–598.
11 Sines, G. (1959) *Metal Fatigue*. McGraw-Hill, NY, USA.
12 Walker, K. (1970) The effect of stress ratio during crack propagation and fatigue for 2024-T3 and 7075-T6 aluminum. In: *Effects of Environment and Complex Load History on Fatigue Life*, ASTM STP 462, American Society for Testing Materials, West Conshohocken, PA, USA, pp. 1–14.
13 Dowling, N. E. (1998) *Mechanical Behavior of Materials*, 2nd edn. Prentice-Hall, Upper Saddle River, NJ, USA.
14 Smith, J. O. (1942) *The Effect of Range of Stress on the Fatigue Strength of Metals*, Engineering Experiment Station Bulletin no. 334, University of Illinois, Urbana, IL, USA.
15 Smith, K. N., Watson, P. and Topper, T. H. (1970) A stress–strain function for the fatigue of metals. *J. Mater.* **5**, 767–778.
16 Pilkey, W. D. and Peterson, R. E. (1997) *Peterson's Stress Concentration Factors*, 2nd edn. Wiley, NY, USA.